Complexity equals anything can grow forever in de Sitter space

Sergio E. Aguilar-Gutierrez,[1,*] Michal P. Heller,[2,†] and Silke Van der Schueren[2,‡]

[1]*Institute for Theoretical Physics, KU Leuven, 3001 Leuven, Belgium*
[2]*Department of Physics and Astronomy, Ghent University, 9000 Ghent, Belgium*

(Received 27 July 2023; accepted 15 July 2024; published 12 September 2024)

Recent developments in anti–de Sitter holography point towards the association of an infinite class of covariant objects, the simplest one being codimension-one extremal volumes, with quantum computational complexity in the microscopic description. One of the defining features of these gravitational complexity proposals is describing the persistent growth of black hole interior in classical gravity. It is tempting to assume that the gravitational complexity proposals apply also to gravity outside their native anti–de Sitter setting in which case they may reveal new truths about these cases with much less understood microscopics. Recent first steps in this direction in de Sitter static patch demonstrated a very different behavior from anti–de Sitter holography deemed hyperfast growth; diverging complexification rate after a finite time. We show that this feature is not a necessity and among gravitational complexity proposals there are ones, that predict linear or exponential late-time growth behaviors for complexity in de Sitter static patches persisting classically forever.

DOI: 10.1103/PhysRevD.110.066009

I. INTRODUCTION AND SUMMARY

Understanding de Sitter (dS) space holography at a level comparable to AdS/CFT [1–3] is an important open question in quantum gravity dating back to the early days of AdS/CFT [4–6].

Key drivers of progress in anti–de Sitter (AdS) quantum gravity have been ideas native to quantum information theory and quantum computing, see e.g., [7–12] for reviews. In recent years these tools have started being applied also to positively curved universes, see e.g., [13–16]. The focal object in the present article is holographic complexity, which arose as a conjectured geometric counterpart of the hardness of dual state or operator preparation using limited resources on the boundary of AdS/CFT [9,12,17]. Considerations based on quantum circuit models of the boundary Hamiltonian time evolution led to two defining features of such geometric quantities in AdS black hole spacetimes: late-time linear growth with time and switchback effect accounting for a delay in the late-time growth due to external perturbations (shock waves). Between 2014 and 2016 three such geometric quantities were identified and thoroughly studied over the past decade; codimension-one boundary-anchored maximal volume slices (CV) [18], gravitational action in the Wheeler-de Witt patch (CA) [19], and spacetime volume of the Wheeler-de Witt patch (CV2.0) [20].

The approach to dS holography that is relevant for our article is the stretched horizon one [14,15,21–26]. It can be thought of to mimic AdS holography in the native to holographic complexity setting of eternal AdS Schwarzschild black holes [27]. The exterior of the latter corresponds to two dS static patches and the AdS asymptotic boundary is mimicked by two stretched horizons, see Fig. 1. Since holographic complexity proposals are geometric constructs, there are no fundamental obstacles to studying them also in this setting. Indeed, over the course of the past two years first CV in two spacetime dimensions [14,28,29] and subsequently in [30] also CV, CA, and CV2.0 in quite a generality were studied in dS stretched horizon holography, see also [31–34] for related recent developments. The common outcome of these studies is holographic complexity diverging (its time derivative diverging in two-dimensional dS) after a finite stretched horizon time. This hyperfast growth [14] is in stark contrast with predictions of holographic complexity proposals for AdS black holes exhibiting a persistent linear growth at a classical level consistent with a local quantum circuit model and might signal a very nonlocal nature of stretched horizon degrees of freedom.

In parallel to the first works studying holographic complexity in dS, it was realized that the space of holographic complexity proposals contains infinitely many members [35,36]. Such Complexity = Anything proposals

*Contact author: sergio.ernesto.aguilar@gmail.com
†Contact author: michal.p.heller@ugent.be
‡Contact author: silkevdschueren@gmail.com

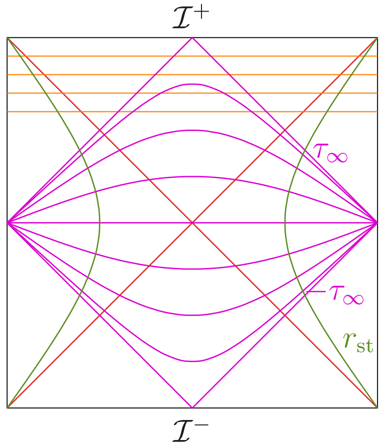

FIG. 1. Penrose diagram of dS_{d+1} space, where the stretched horizon is shown in green at $r_{\rm st}$ and the extremal volumes of the CV proposal in pink. The origin of the hyperfast growth is approaching the infinity touching light cone in finite stretched horizon time (i.e., at τ_∞ and $-\tau_\infty$). In orange, we display slices of constant global time, which exhibit persistent growth as they avoid future infinity. The key idea of our paper is to find analogous slices, but belonging to CAny and understand their properties.

(CAny) are defined by obeying the late-time linear growth and switchback effect for AdS black holes and can be defined by codimension-one as well as codimension-zero geometric objects. However, *a priori* it is not guaranteed that their other behaviors, in particular in dS, will also be shared with CV, CA, and CV2.0. This leads to our motivating question:

> Assuming stretched horizon holography and holographic complexity proposals is the hyperfast growth as universal for dS holographic complexities as linear growth and switchback for AdS ones?

Contrary to expectations stemming from the accelerated expansion of dS universes, our work demonstrates that hyperfast growth is not a necessity within CAny proposals, but a feature appearing for some of them, with different kinds of growth present for another subset. We demonstrate this using a family of CAny proposals defined on constant mean curvature (CMC) spatial slices with our arguments covering also Schwarzschild dS black holes (SdS). However, these proposals might not describe holographic complexity as it is defined in the AdS context; instead, they are general observables of interest for static patch holography in dS space. An interpretation of holographic complexity in dS space would require developing a quantum circuit interpretation of its quantum mechanical dual theory, which is still missing. The most promising case is certainly a two-dimensional one, where on one hand our findings apply and, on the other, an expanding patch of a dS geometry can be embedded outside a horizon in an AdS spacetime subject then to more standard holographic interpretations [28,37–39]. Our perspective is, however, to develop geometric intuitions about what is possible for holographic complexity rather than to provide a microscopic interpretation, which apart from one isolated case [40] has not been settled in a precise manner.

Finally, our considerations of holographic complexity in dS universes bear implications on a subclass of CAny holographic complexity proposals in AdS utilizing CMC spatial slices. To this end, we observe that complexity interpretation in eternal AdS black hole spacetimes may generically require an additional ingredient in these CAny proposals that renders their time evolution symmetric.

II. SETUP

The asymptotically dS geometries of interest in $d+1$ spacetime dimensions are described by the metric,

$$\mathrm{d}s^2 = -f(r)\mathrm{d}t_{L/R}^2 + \frac{\mathrm{d}r^2}{f(r)} + r^2\mathrm{d}\Omega_{d-1}^2, \qquad (1)$$

where

$$f(r) = 1 - r^2 - \frac{2\mu}{r^{d-2}} \qquad (2)$$

and $\mathrm{d}\Omega_{d-1}^2$ is the metric on a unit $(d-1)$-dimensional sphere. Meanwhile, the (dimensionless) parameter μ,

$$\mu \in [0, \mu_N], \qquad \mu_N \equiv \frac{1}{d}\left(\frac{d-2}{d}\right)^{\frac{d-2}{2}}. \qquad (3)$$

allows us to study spacetimes from the empty dS ($\mu = 0$) all the way to the Nariai black hole space ($\mu = \mu_N$), i.e., the largest black hole that can fit in dS space. Note that in this paper we set the curvature scale associated with a cosmological constant (both positive and negative) to unity. The coordinates (1) are Schwarzschild coordinates and cover the region outside the horizon (the static patch for dS), hence the presence of two-time variables, one for each exterior.

In analogy with AdS holography [27] and following [14,28–30], we will be interested in introducing stretched horizons at $r = r_{\rm st}$ with constant t_L and t_R slices thereof defining states in a putative microscopic description involving two Hilbert spaces, one for each stretched horizon. We orient both time directions to increase towards future infinity and consider left-right symmetric time evolution in $t_L = t_R \equiv \frac{t}{2}$. The venerable CV proposal amounts to finding stretched horizon anchored codimension-1 volumes and studying them as a function of t. Since this and any other holographic complexity proposal require connecting two boundaries through an inflating region complementary to the static patch, in explicit calculations we will be using ingoing Eddington-Finkelstein (EF) coordinates given by

$$\mathrm{d}s^2 = -f(r)\mathrm{d}v^2 + 2\mathrm{d}v\mathrm{d}r + r^2\mathrm{d}\Omega_{d-1}^2. \tag{4}$$

Because of the left-right symmetry, it will be enough to consider only one patch of such coordinates.

III. KEY IDEA

Figure 1 depicts the outcome of CV calculating in stretched horizon dS holography from [14,28–30]. Similar considerations apply to CA and CV2.0. What one sees is that extremal volume slices cease to exist for large or small enough t on the stretched horizon. This occurs because as a result of extremization the outermost CV carriers approach and touch future or past infinity. In $d = 1$ this implies a singular derivative of the complexity with respect to t and in $d \geq 2$ this implies on top of a divergence of complexity itself, which is the precise statement of the hyperfast growth.

In dS or SdS geometry, there are infinitely many other spatial slices that do not exhibit hyperfast growth. For example, constant global time slices of dS depicted with orange in Fig. 1 exhibit persistent exponential growth at late times. Of course, at this level, such slices are not covariantly defined and it is not clear if their volumes arise from a particular CAny proposal.

The key idea in the present paper is to find a family of codimension one objects that avoid the future infinity (to start with, and later also the past infinity) in a similar manner as orange slices do in Fig. 1, which fall into the class of CAny proposals.

As it turns out, we do not have to search far; CMC slices that appeared earlier in the context of holographic complexity in [36,41,42] will have precisely the desired property. Such slices will bend towards the past or future light cone as their curvature, respectively, increases or decreases. Then, there should exist a class of holographic complexity notions that without fine-tuning avoids the hyperfast growth associated with touching $\mathcal{I}^+$ or $\mathcal{I}^-$, or at best both, rendering the observables finite during the time evolution.

IV. THE RELEVANT CLASS OF COMPLEXITY PROPOSALS

CAny proposals [35,36] are defined in a two-step procedure. First one defines a boundary (stretched horizon) anchored geometric region using extremization and, subsequently, one characterizes it in terms of, in general, another geometric functional yielding a non-negative number—a value of holographic complexity. Of course, the challenge lies in carving out the space of such functionals, which gives rise to the linear growth and the switchback effect for AdS black holes. What is known so far are several classes of objects specified by continuous parameters for which these properties have been demonstrated.

In our work, we will be interested in (spatial) volumes of stretched horizon-anchored CMC slices. Maximal volume slices giving rise to CV fall into this class, but we will be clearly interested in other members. Along the lines of CAny, they can be obtained by extremizing,

$$\mathcal{C}_{\mathrm{CMC}} = \frac{1}{G_N}\left[\alpha_+ \int_{\Sigma_+} \mathrm{d}^d\sigma_+ \sqrt{h} + \alpha_- \int_{\Sigma_-} \mathrm{d}^d\sigma_- \sqrt{h} \right. \\ \left. + \alpha_B \int_{\mathcal{M}} \mathrm{d}^{d+1}x \sqrt{-g}\right], \tag{5}$$

where $\mathcal{M}$ is the codimension-zero bulk region that in the end will play no role; $\Sigma_\pm$ are its, crucial for us, future and past boundaries with general coordinates $\sigma_\pm$ and $\alpha_\pm$, α_B are positive constants.

The extremization of (5) confirms $\Sigma_\pm$ are CMC slices,

$$K|_{\Sigma_\epsilon} = -\epsilon \frac{\alpha_B}{\alpha_\epsilon}, \qquad \epsilon = \pm, \tag{6}$$

where K is the trace of the extrinsic curvature with normal vectors to both $\Sigma_\pm$ chosen to be future oriented.

Our CAny complexity carrier will be

$$\mathcal{C}^\epsilon \equiv \frac{1}{G_N}\int_{\Sigma_\epsilon} \mathrm{d}^d\sigma_\epsilon \sqrt{h}, \tag{7}$$

where we are free to pick either Σ_+ or Σ_-. The results of [36] guarantee that (7) is a valid CAny proposal.

V. LATE TIME GROWTH

The evaluation of the volume (7) of the CMC slice Σ_ϵ can be recast as [42],

$$\mathcal{C}^\epsilon = \frac{2\Omega_{d-1}}{G_N}\int_{r_{\mathrm{st}}}^{r_t} \frac{r^{2(d-1)}\mathrm{d}r}{\sqrt{-\mathcal{U}(P_v^\epsilon, r)}}, \tag{8}$$

where P_v^ϵ is the conserved momentum in an analog particle motion problem,

$$\mathcal{U}(P_v^\epsilon, r) = -f(r)r^{2(d-1)} - \left(P_v^\epsilon - |K|\frac{\epsilon}{d}r^d\right)^2 \tag{9}$$

is the particle's effective potential, whereas $r = r_t$ is the turning point. The latter is the location where $\mathcal{U}(P_v^\epsilon, r_t) = 0$ or in geometric terms it is the tip of CMC [$r'(v) = 0$ there]. We are interested in the time evolution of (7) measured with respect to r_{st}. Using the technology of [35,36] one finds at late times

$$\lim_{t\to\infty}\frac{\mathrm{d}}{\mathrm{d}t}\mathcal{C}^\epsilon = \frac{\Omega_{d-1}}{G_N}\sqrt{-f(r_f)r_f^{2(d-1)}}, \tag{10}$$

where we consider solutions characterized by

$$\lim_{t\to\infty}\frac{\mathrm{d}P_v^\epsilon}{\mathrm{d}t}=0 \tag{11}$$

and $r_f \equiv \lim_{t\to\infty} r_t$ is the final value of the turning point. Notice that (10) does not depend on the particular value of $r_{\rm st}$. Condition (11) can also be reformulated as finding the maximum of the potential (9),

$$\mathcal{U}|_{r_f}=0, \qquad \partial_r\mathcal{U}|_{r_f}=0, \qquad \partial_r^2\mathcal{U}|_{r_f}\leq 0. \tag{12}$$

We may define a function,

$$H(r,K)=4rf(r)((d-1)f'(r)+K^2r)+4(d-1)^2f(r)^2 + r^2f'(r)^2, \tag{13}$$

where the relations (12) imply that late time growth of (9) with (5) is achieved when one can find the roots of

$$H(r_f,K)=0, \tag{14}$$

for some choice of K. We now specialize in asymptotically dS backgrounds, employing the factor (2). We discuss different cases under our proposal.

(i) Empty dS space, $\mu=0$,

$$r_f^2=\frac{K^2-2d(d-1)\pm|K|\sqrt{K^2-4(d-1)}}{2(K^2-d^2)}. \tag{15}$$

Then, in order to have at least one turning point at late times, $r_f\in\mathbb{R}$, in empty dS space with $d\geq 2$ spatial dimensions, we find

$$|K|\geq K_{\rm crit,dS}=2\sqrt{d-1}. \tag{16}$$

The CMC slices obeying this bound are displayed in Fig. 2. However, notice that the relation (16) is not valid when $d=1$, since for $d=1$, $|K|<1$ Eq. (15) does not have a valid solution; instead one finds $K\geq 1$ for the CMC slices to evolve at arbitrarily late times.

(ii) For the Nariai black hole spacetime, $\mu=\mu_N$, one finds that $f(r_f)=f'(r_f)=0$ at the location,

$$r_f=\sqrt{\frac{d-2}{d}}, \tag{17}$$

such that the turning point coincides with the cosmological horizon. However, for r_f to be the final slice, it also needs to be a maximum of the potential $\mathcal{U}(P_v^\epsilon,r)$ in (9), which leads to

$$|K|\geq K_{\rm crit,N}\equiv\sqrt{d}. \tag{18}$$

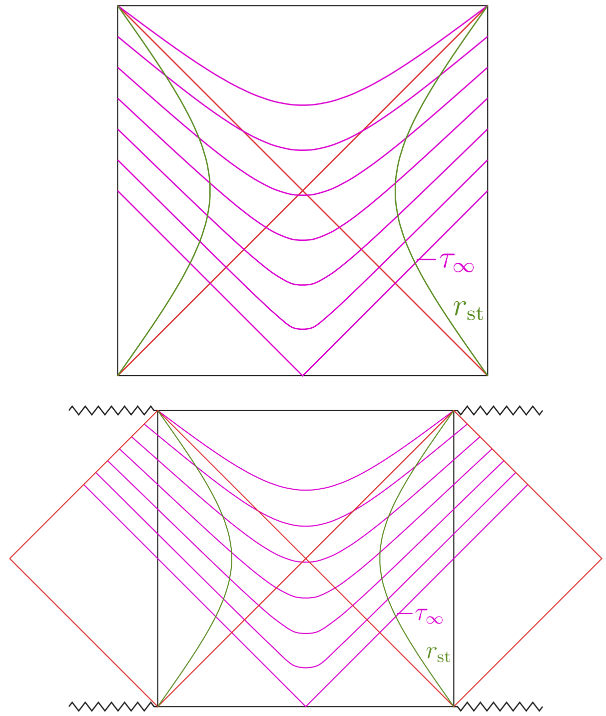

FIG. 2. CMC slices for $K\geq K_{\rm crit,dS}$ in empty dS_{d+1} space (above) and SdS_{d+1} (below). All the slices remain bounded below $\mathcal{I}^+$ and the corresponding complexity observable (8) generically displays a late-time linear growth (10), except for some fine-tuned situations discussed in the main text. The solutions with $K<0$ can be obtained by a top-bottom reflection.

(iii) For generic μ, one cannot derive closed-form solutions for r_f in (13), except for the SdS_3 space, which is locally identical to dS_3. We explicitly find that (16) is always respected in such a case. For higher dimensions and generic μ, the bounds on $|K|$ will lay between (16) and (18) [43]. Such black holes are unstable and decay in empty dS_{d+1} space [44]. The analysis for generic Reissner-Nordström-de Sitter (RNdS) black holes is shown in Appendix.

Note that the solutions for (15) in $d=1$ and $d=2$ as well as for SdS_3, lead to $r_f\to\infty$ when $|K|=K_{\rm crit}$. We find exponential growth for (8) in these two very special cases. For $d=3$ and higher we find finite r_f for $K=K_{\rm crit}$, which translates to the linear growth.

VI. RESTORING TIME SYMMETRY

Although the rate of growth of the observables in (7) evaluated on the CMC slices asymptotes to a constant value at late times (10) when $K>K_{\rm crit}$ the CMC slices still hit $\mathcal{I}^-$ at minus the critical time, as illustrated in Fig. 2. This produces hyperfast behavior in the past. The opposite case occurs by symmetry for $K<-K_{\rm crit}$.

A natural way to restore time-reversal symmetry in the observables is to modify the second step of the CAny

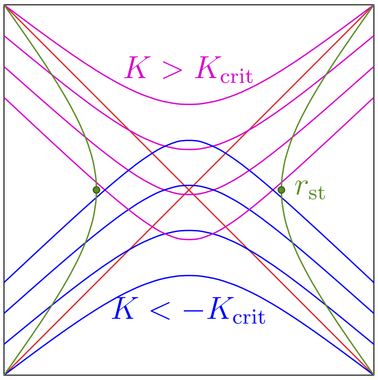

FIG. 3. Our time symmetric complexity proposal (19) in empty dS_{d+1} allowing both early- and late-time linear growth. At negative times, the CMC with $K < -K_{\rm crit}$ dominates, shown in blue; while at positive times, the CMC with $K > K_{\rm crit}$ dominates. The exchange of dominance at $t = 0$ between CMC slices is indicated by the green dots on the stretched horizon.

prescription so that it selects the result with the minimal value among the slices with a given value for $|K|$,

$$\mathcal{C}_{\rm sym} = \min_{\epsilon=+,-} \mathcal{C}^{\epsilon}. \tag{19}$$

The minimization is performed over the existing slices, so technically it is only a minor modification. This procedure does not alter the conclusion that the constructed covariant notions are complexity proposals, as the linear growth and the switchback effect for AdS black holes remain present. We show this explicitly in the Appendix.[1] As a result, this idea can be thought of as a further enlargement of the space of CAny proposals and might even be advantageous when considering more complicated black holes in AdS.

In the dS case, our improved proposal (19) will receive a contribution from a slice with $K < 0$ at early times, and $K > 0$ at late times, as shown in Fig. 3. A potential subtlety with this generalization is that the complexity growth rate (10) might become discontinuous at the time when the change of CMC slice occurs. However, this is in principle allowed in the definition of holographic complexity proposals [35,36]. Indeed, the CA proposal applied to a three-dimensional AdS black hole generically exhibits the same kind of behavior [45].

VII. DISCUSSION

Our paper demonstrates that the hyperfast growth of holographic complexity in asymptotically dS spacetimes, as found earlier in the CV, CA, and CV2.0 proposals, is not a universal feature in the CAny landscape. Employing volumes of codimension-one CMC slices, being members of CAny family, we show that holographic complexity can exhibit persistent linear or exponential growth in asymptotically dS universes. Physically, this exponential behavior occurs when the final slice asymptotes the future/past infinity of the inflating region. While a linear growth can be also obtained upon cutting out the dS geometry past some late time slice [30], we obtained it without modifying dS geometry in any way.

From the perspective of dS holography, it is tempting to speculate that the presence or the absence of hyperfast growth is related to the choice of a penalty schedule in the microscopic definition of complexity, i.e., different designations which operations are hard and which are easy to implement. It would be interesting to study it, as well as the protocol in (19), in either a class SYK models associated with JT gravity with positive cosmological constant [46–49] or in quantum circuit toy models of de Sitter space [50–53].

More along these lines, specializing in CV proposal in two spacetime dimensions, where the complexity carriers are geodesics, it is known that in dS past the critical time on a stretched horizon, there are no spatial geodesics. However, using a closed-form expression for a geodesic distance one obtains an answer with both real and imaginary parts [54,55]. While one may speculate about nonorthodox interpretation in terms of complexity, e.g., with real part accounting for unitary and imaginary part for possible nonunitary gates, we find it important to stress that our final result (19) does not require any departure from a standard counting interpretation of unitary gates.

Furthermore, the space of CAny proposals is vast, and arguably one of the main open problems for the field of holographic complexity is to study it in a more systematic manner. To this end, our results show the existence of a so far unrecognized structure in the CAny landscape stemming from the presence (so far demonstrated for CV, CA, and CV2.0) or the absence of the hyperfast growth demonstrated here for CMC complexity carriers. One intriguing future research direction would be to find more members of the hyperfast growth escaping CAny proposals and, another, to seek other structures present. On the former front, we want to emphasize that there is a continuum of CAny proposals that do not exhibit hyperfast growth, as encapsulated by (16).

We also want to highlight a potentially puzzling feature for a class of CAny proposals we considered, which to the best of our knowledge has not been previously seen in the literature. As illustrated in Fig. 2, asymmetric time evolution may occur such that hyperfast growth is observed in the past or future, while the linear or exponential growth remains for the late or early time regime respectively. If we want to assign a Nielsen unitary complexity [12,56] interpretation to this setting, then the complexity of a unitary is the same as its inverse. This implies time asymmetric quantities in time-symmetric setups either do not capture (this type of) complexity or the considered time evolution is not unitary. The same occurs for CAny proposals on CMC slices even for AdS planar black holes

[1]One of the authors has recently shown that this class of proposals also satisfies the switchback effect in SdS space [43].

with the location of the early/late turning point not being time-reflection symmetric.

The time symmetry in the observables can be restored by introducing a covariant protocol that alternates between CMC slices of opposing sign, where the slice that minimizes complexity is chosen. This consideration led us to a new CAny proposal encapsulated by (19), which is time-symmetric. Notice, however, that we could have chosen instead a protocol maximizing complexity over CMC slices, or even averaging, instead of doing the minimization that we proposed. However, in such cases, the hyperfast growth would not be avoided anymore.

Finally, let us reiterate that the defining features for CAny proposals are the late-time linear growth and the switchback effect for AdS black holes. If one were to add to this list the hyperfast growth in dS, our paper could be then viewed as ruling out a subclass of CAny proposals.

ACKNOWLEDGMENTS

We would like to thank Stefano Baiguera, Damián Galante, Eivind Jørstad, Ayan K. Patra, Juan F. Pedraza, Leonard Susskind, Qi-Feng Wu, and Nicolò Zenoni for useful discussions on de Sitter space and complexity, and Alexandre Serantes for a collaboration on a related topic. S. E. A. G. thanks the University of Amsterdam and the Delta Institute for Theoretical Physics for their hospitality and support during the research. The work of S. E. A. G. is partially supported by the FWO Research Project No. G0H9318N and the interuniversity Project No. iBOF/21/084.

APPENDIX A: LATE TIME GROWTH IN REISSNER-NORDSTRÖM-DE SITTER SPACE

We consider a generalization of the previous analysis for electrically or magnetically charged black holes in asymptotically dS space, known as the RNdS space. The blackening factor in $(d+1)$-dimensions in (2) is modified to

$$f(r) = 1 - r^2 - \frac{2\mu}{r^{d-2}} + \frac{q^2}{r^{2(d-2)}}, \tag{A1}$$

where, q is a parameter related to the electric or magnetic charge of the black hole, which we will consider $q > 0$ through the discussion. The three positive roots of (A1) for $d > 2$ represent the inner and outer black hole horizon, as well as the cosmological horizon; however, the real solutions are only present when there are bounds on the parameters μ and q. There exists a black hole with maximal mass and charge parameters, $\mu = \mu_U$ and $q = q_U$ respectively, denoted as the ultracold (U) solution, for which [57]

$$\mu_U = \frac{2}{d}\left(\frac{(d-2)^2}{d(d-1)}\right)^{\frac{d-2}{2}}, \qquad q_U = \frac{1}{\sqrt{d-1}}\left(\frac{(d-2)^2}{d(d-1)}\right)^{\frac{d-2}{2}}. \tag{A2}$$

In these conditions, the outer, inner, and cosmological horizons have the same radius, r_U, for which

$$f(r_U) = f'(r_U) = f''(r_U) = 0, \qquad r_U = \frac{d-2}{\sqrt{d(d-1)}}, \tag{A3}$$

which indicates that $r_f = r_U$ is a root for (13). Moreover, there are no bounds for $|K|$ resulting from the conditions (12) in this limit.

We will evaluate $H(r, K)$ in (13) with the roots in (15) and (17) while keeping the mass and charge of the black hole arbitrary. Defining $m \equiv \mu/\mu_U$ and $\rho \equiv q/q_U$, one might express,

$$\begin{aligned} H(r_f^{(\mathrm{dS})}, K_{\mathrm{crit,dS}}) = {} & 4(4(d-2)^{3(d-2)} d^{2-d}(d-1)^{4-2d}(m^2+\rho^2) - 4(d-2)^{\frac{9(d-2)}{2}} d^{3-\frac{3d}{2}}(d-1)^{5-3d} m\rho^2 \\ & - 8(d-2)^{\frac{3(d-2)}{2}} d^{-d/2}(d-1)^{3-d} m + (d-2)^{6(d-2)} d^{4-2d}(d-1)^{6-4d}\rho^4), \end{aligned} \tag{A4}$$

$$\begin{aligned} H(r_f^{(\mathrm{N})}, K) = {} & \frac{4}{(d-1)^2 d^2}(4d^4(m-1)^2 + d^3(K^2(-4m+\rho^2+3) - 4(m-1)(2m+\rho^2-3)) + 16K^2(m-1) \\ & + d^2(4K^2(5m-\rho^2-4) + (2m+\rho^2-3)^2) + 4dK^2(-8m+\rho^2+7)). \end{aligned} \tag{A5}$$

We deduce that (A4) is negative for all $d \geq 3$ for the allowed parameter space of $m, q \in (0,1)$, while (A5) is positive. Moreover, $H(r_f^{(\mathrm{dS})}, K)$ becomes more negative as we increase $|K| > K_{\mathrm{crit,dS}}$. Then, according to the intermediate value theorem, there will exist at least a real root $r_f \in [r_f^{(\mathrm{dS})}, r_{\mathrm{U}}]$ for general RNdS_{d+1} space.

APPENDIX B: SWITCHBACK EFFECT IN ASYMPTOTICALLY ADS PLANAR BLACK HOLES

In this Appendix we show that the CAny proposals in (5) and (7) reproduce the switchback effect in AdS planar black holes. The late-time linear growth property for the proposals under consideration has been studied in [36,42].

The asymptotically AdS_{d+1} planar black hole metric can be expressed as

$$\mathrm{d}s^2 = -f(r)\mathrm{d}t^2 + \frac{\mathrm{d}r^2}{f(r)} + r^2\mathrm{d}\vec{x}^2,$$
$$f(r) = r^2\left(1 - \frac{r_h^d}{r^d}\right), \tag{B1}$$

where r_h is the location of the black hole horizon, and $\vec{x}$ a $(d-1)$-dimensional vector.

We will consider a coordinate transformation from the EF to Kruskal coordinates, which we define by

$$U = \mathrm{e}^{-\frac{f'(r_h)}{2}u}, \qquad V = -\mathrm{e}^{\frac{f'(r_h)}{2}v}. \tag{B2}$$

The geometry for shockwave perturbations sent along $U = 0$ as [35,36] can be then described as

$$\mathrm{d}s^2 = -2A(U[V + \alpha_i\Theta(U)])\mathrm{d}U\mathrm{d}V + B(U[V + \alpha_i\Theta(U)])\mathrm{d}\vec{x}^2, \tag{B3}$$

where

$$A(UV) \equiv -\frac{2}{\mathrm{UV}}\frac{f(r)}{f'(r_h)^2}, \qquad B(UV) \equiv r^2, \tag{B4}$$

$$\alpha_i = 2\mathrm{e}^{-\frac{f'(r_h)}{2}(t_*^{(\mathrm{b})} \pm t_i)}. \tag{B5}$$

Here, t_i, with $i \in 1, \ldots n$, are the shockwave insertion times with respect to the asymptotic boundary, where we will consider the total number of shockwaves n to be even; the $\pm$ sign indicates the direction that the shockwaves are sent to and $t_*^{(\mathrm{b})}$ is the scrambling time of the AdS black hole. We are interested in an alternating order for the insertion times, i.e.,

$$t_{2k+1} > t_{2k}, \qquad t_{2k} < t_{2k-1}, \tag{B6}$$

where $k \in 1, \ldots, n/2$. Moreover, we consider the shockwave regime where $|t_{i+1} - t_i| \gg t_*^{(\mathrm{b})}$. Under these conditions, one may express the complexity in the alternating shockwave as [35,36]

$$\mathcal{C}^\epsilon(t_L, t_R) = \mathcal{C}^\epsilon(t_R, V_1) + \mathcal{C}^\epsilon(V_1 + \alpha, U_2) + \cdots + \mathcal{C}^\epsilon(U_{n-1} - \alpha_{n-1}, V_n) + \mathcal{C}^\epsilon(V_{n-1} + \alpha_{n-1}, t_L), \tag{B7}$$

where $\mathcal{C}^\epsilon(\cdot,\cdot)$ denotes the contributions from Σ_ϵ with two fixed endpoints and all endpoints are located either on the left/right event horizon (r_h) or asymptotic infinity. The different cases are illustrated in Fig. 4.[2]

The different contributions in (B3) can be expressed with EF coordinates (4) and considering symmetric time evolution $t_L = t_R = t/2$ as

$$\mathcal{C}^\epsilon(t_R, V_L) = \mathcal{C}^\epsilon(V_R, t_L) = -\frac{\mathcal{V}_x}{G_N}a(r_t)\sqrt{-f(r_t)r_t^{2(d-1)}}\left(\int_{r_t}^{r_{\mathrm{bdy}}} + \int_{r_t}^{r_h}\right)\frac{(P_v^\epsilon + \frac{\epsilon L|K|}{d}r^d)\mathrm{d}r}{f(r)\sqrt{-\mathcal{U}(P_v^\epsilon, r)}},$$
$$\mathcal{C}^\epsilon(V_R, U_L) = -\frac{2\mathcal{V}_x}{G_N}a(r_t)\sqrt{-f(r_t)r_t^{2(d-1)}}\int_{r_t}^{r_h}\frac{(P_v^\epsilon + \frac{\epsilon L|K|}{d}r^d)\mathrm{d}r}{f(r)\sqrt{-\mathcal{U}(P_v^\epsilon, r)}}, \tag{B8}$$

where r_{bdy} represents a cutoff radial location of the asymptotic boundary. One can perform a very similar analysis of the time dependence of the CAny proposals in (5), (7) to the one in the main text. One of the differences, however, is that the effective potential $\mathcal{U}(P_v^\epsilon, r)$ in (9) has a modification $K \to -K$ [36]. Denoting again $K|_{\Sigma_+} = -|K|$ and $K|_{\Sigma_-} = |K|$, we have

$$\mathcal{U}(P_v^\epsilon, r) \equiv -f(r)r^{2(d-1)} - \left(P_v^\epsilon + \epsilon\frac{|K|}{d}r^d\right)^2. \tag{B9}$$

To study the complexity growth evolution in the perturbed geometry, we must also evaluate its dependence on the location $u_{R,L}$, $v_{R,L}$ where Σ_ϵ intersects with the left/right horizon r_h. In this case, we derive

$$v_R - v_t = \int_{r_t}^{r_h}\frac{\mathrm{d}r}{f(r)}\left(1 - \frac{P_v^\epsilon + \frac{\epsilon|K|}{d}r^d}{\sqrt{-\mathcal{U}(P_v\epsilon, r)}}\right), \tag{B10}$$

where $v_t = v_R(r_t)$.

We may also perform the expansion around the final slice where (12) allows us to approximate

$$\lim_{r\to r_f} U(P_v^\epsilon, r) \simeq \frac{1}{2}(r - r_f)^2\mathcal{U}''(P_v^\epsilon, r) + \mathcal{O}(|r - r_f|^3). \tag{B11}$$

The CAny proposal near the final turning point r_f then can be evaluated as follows:

[2] In the following, we will work in scaled coordinate where the AdS scale $\ell_{\mathrm{AdS}} = 1$.

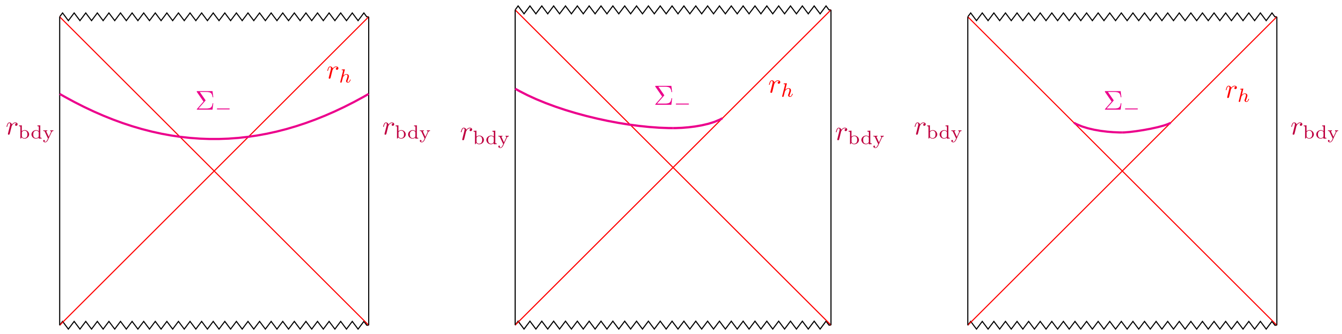

FIG. 4. Extremal complexity surface Σ_ϵ (pink) in (B7) for $\epsilon = -$ in a planar AdS black hole. *Left*: $\mathcal{C}^-(t_L, t_R)$; *Center*: $\mathcal{C}^-(V_R, t_L)$; and *Right*: $\mathcal{C}^-(V_R, U_L)$. $r_{\rm bdy}$ (purple) denotes the radial cutoff of the asymptotic boundary, and r_h (red) the event horizon.

$$\mathcal{C}^\epsilon(V_R, U_L) = \frac{\mathcal{V}_x}{G_N} P^\epsilon_\infty v, \quad P^\epsilon_\infty = \sqrt{-f(r_f) r_f^{2(d-1)}}, \tag{B12}$$

where r_f is a root of the function in (13).

The result above can be used to evaluate the contributions in (B7) as

$$\mathcal{C}^\epsilon(V_R, t_L) = \frac{\mathcal{V}_x}{G_N} P^\epsilon_\infty \log e^{t_L} V_R, \tag{B13}$$

$$\mathcal{C}^\epsilon(V_R, U_L) = \frac{\mathcal{V}_x}{G_N} P^\epsilon_\infty \log U_L V_R, \tag{B14}$$

$$\mathcal{C}^\epsilon(t_R, V_L) = \frac{\mathcal{V}_x}{G_N} P^\epsilon_\infty \log V_L e^{t_R}. \tag{B15}$$

However, there will also be an early time contribution in the shockwave geometry, given by the term

$$\mathcal{C}^\epsilon(V_L, U_R) = \frac{\mathcal{V}_x}{G_N} P^\epsilon_{-\infty} \log U_L V_R, \tag{B16}$$

where

$$P^\epsilon_{-\infty} = \lim_{t\to-\infty} \sqrt{-f(r_I) r_I^{2(d-1)}}, \tag{B17}$$

and $r_I = \lim_{t\to-\infty} r_t$, for which there is a sign flip in $K \to -K$. Using the blackening factor (B1), we explicitly find that $P^\epsilon_\infty = P^\epsilon_{-\infty}$. (B7) then transforms into

$$\mathcal{C}^\epsilon(t_L, t_R) \simeq \frac{\mathcal{V}_x P^\epsilon_\infty}{G_N} [U_1 e^{t_R} + \log(U_1 - \alpha) V_2 + \cdots + \log((V_n + \alpha_n) e^{t_L})]. \tag{B18}$$

Extremizing (B18) with respect to an arbitrary interception point (V_i, U_i) in the multiple shockwave geometry,

$$\frac{d\mathcal{C}^\epsilon(t_L, t_R)}{dV_i} = 0, \qquad \frac{d\mathcal{C}^\epsilon(t_L, t_R)}{dU_i} = 0, \tag{B19}$$

leads us to the location

$$V_i = -\frac{\alpha_i}{2}, \qquad U_i = \frac{\alpha_i}{2}. \tag{B20}$$

Replacing the interception points into (B18) generates,

$$\mathcal{C}^\epsilon \simeq \frac{\mathcal{V}_x P^\epsilon_{+\infty}}{G_N} \left(t_R + t_L + 2\left(\sum_{k=1}^n t_k - n t_*^{(b)} \right) \right), \tag{B21}$$

where the result is expressed up to the addition of constant terms. Given the ordering of the insertion times, we reproduce the switchback effect property [35,36],

$$\mathcal{C}^\epsilon \propto |t_R + t_1| + |t_2 - t_1| + \cdots + |t_n - t_L| - 2n t_*^{(b)}. \tag{B22}$$

Notice that the minimization protocol introduced in (19) does not alter the result above.

[1] J. M. Maldacena, The large N limit of superconformal field theories and supergravity, Adv. Theor. Math. Phys. **2**, 231 (1998).

[2] S. S. Gubser, I. R. Klebanov, and A. M. Polyakov, Gauge theory correlators from noncritical string theory, Phys. Lett. B **428**, 105 (1998).

[3] E. Witten, Anti-de Sitter space and holography, Adv. Theor. Math. Phys. **2**, 253 (1998).

[4] A. Strominger, The dS/CFT correspondence, J. High Energy Phys. 10 (2001) 034.

[5] E. Witten, Quantum gravity in de Sitter space, in *Strings 2001: International Conference* (2001), arXiv:hep-th/0106109.

[6] J. M. Maldacena, Non-Gaussian features of primordial fluctuations in single field inflationary models, J. High Energy Phys. 05 (2003) 013.
[7] D. Harlow, Jerusalem lectures on black holes and quantum information, Rev. Mod. Phys. **88**, 015002 (2016).
[8] M. Rangamani and T. Takayanagi, *Holographic Entanglement Entropy* (Springer, New York, 2017), Vol. 931, 10.1007/978-3-319-52573-0.
[9] L. Susskind, *Three Lectures on Complexity and Black Holes*, SpringerBriefs in Physics (Springer, New York, 2018).
[10] A. Almheiri, T. Hartman, J. Maldacena, E. Shaghoulian, and A. Tajdini, The entropy of Hawking radiation, Rev. Mod. Phys. **93**, 035002 (2021).
[11] B. Chen, B. Czech, and Z.-z. Wang, Quantum information in holographic duality, Rep. Prog. Phys. **85**, 046001 (2022).
[12] S. Chapman and G. Policastro, Quantum computational complexity from quantum information to black holes and back, Eur. Phys. J. C **82**, 128 (2022).
[13] X. Dong, E. Silverstein, and G. Torroba, De Sitter holography and entanglement entropy, J. High Energy Phys. 07 (2018) 050.
[14] L. Susskind, Entanglement and chaos in de Sitter space holography: An SYK example, J. Hologr. Appl. Phys. **1**, 1 (2021).
[15] E. Shaghoulian and L. Susskind, Entanglement in de Sitter space, J. High Energy Phys. 08 (2022) 198.
[16] V. Chandrasekaran, R. Longo, G. Penington, and E. Witten, An algebra of observables for de Sitter space, J. High Energy Phys. 02 (2023) 082.
[17] L. Susskind, Computational complexity and black hole horizons, Fortschr. Phys. **64**, 44 (2014).
[18] D. Stanford and L. Susskind, Complexity and shock wave geometries, Phys. Rev. D **90**, 126007 (2014).
[19] A. R. Brown, D. A. Roberts, L. Susskind, B. Swingle, and Y. Zhao, Holographic complexity equals bulk action?, Phys. Rev. Lett. **116**, 191301 (2016).
[20] J. Couch, W. Fischler, and P. H. Nguyen, Noether charge, black hole volume, and complexity, J. High Energy Phys. 03 (2017) 119.
[21] L. Susskind, Scrambling in double-scaled SYK and de Sitter space, arXiv:2205.00315.
[22] H. W. Lin, The bulk Hilbert space of double scaled SYK, J. High Energy Phys. 11 (2022) 060.
[23] H. Lin and L. Susskind, Infinite temperature's not so hot, arXiv:2206.01083.
[24] B. Bhattacharjee, P. Nandy, and T. Pathak, Krylov complexity in large q and double-scaled SYK model, J. High Energy Phys. 08 (2023) 099.
[25] L. Susskind, De Sitter space has no chords. Almost everything is confined, J. Hologr. Appl. Phys. **3**, 1 (2023).
[26] L. Susskind, A paradox and its resolution illustrate principles of de Sitter holography, arXiv:2304.00589.
[27] J. M. Maldacena, Eternal black holes in anti-de Sitter, J. High Energy Phys. 04 (2003) 021.
[28] S. Chapman, D. A. Galante, and E. D. Kramer, Holographic complexity and de Sitter space, J. High Energy Phys. 02 (2022) 198.
[29] D. Galante, Geodesics, complexity and holography in (A)dS_2, Proc. Sci., CORFU2021 (**2022**) 359.
[30] E. Jørstad, R. C. Myers, and S.-M. Ruan, Holographic complexity in dS_{d+1}, J. High Energy Phys. 05 (2022) 119.
[31] R. Auzzi, G. Nardelli, G. P. Ungureanu, and N. Zenoni, Volume complexity of dS bubbles, Phys. Rev. D **108**, 026006 (2023).
[32] T. Anegawa, N. Iizuka, S. K. Sake, and N. Zenoni, Is action complexity better for de Sitter space in Jackiw-Teitelboim gravity?, J. High Energy Phys. 06 (2023) 213.
[33] T. Anegawa and N. Iizuka, Shock waves and delay of hyperfast growth in de Sitter complexity, J. High Energy Phys. 08 (2023) 115.
[34] S. Baiguera, R. Berman, S. Chapman, and R. C. Myers, The cosmological switchback effect, J. High Energy Phys. 07 (2023) 162.
[35] A. Belin, R. C. Myers, S.-M. Ruan, G. Sárosi, and A. J. Speranza, Does complexity equal anything?, Phys. Rev. Lett. **128**, 081602 (2022).
[36] A. Belin, R. C. Myers, S.-M. Ruan, G. Sárosi, and A. J. Speranza, Complexity equals anything II, J. High Energy Phys. 01 (2023) 154.
[37] D. Anninos and D. M. Hofman, Infrared realization of dS_2 in AdS_2, Classical Quantum Gravity **35**, 085003 (2018).
[38] D. Anninos and D. A. Galante, Constructing AdS_2 flow geometries, J. High Energy Phys. 02 (2021) 045.
[39] F. Ecker, D. Grumiller, and R. McNees, $\mathbf{dS_2}$ as excitation of $\mathbf{AdS_2}$, SciPost Phys. **13**, 119 (2022).
[40] E. Rabinovici, A. Sánchez-Garrido, R. Shir, and J. Sonner, A bulk manifestation of Krylov complexity, J. High Energy Phys. 08 (2023) 213.
[41] A. R. Chandra, J. de Boer, M. Flory, M. P. Heller, S. Hörtner, and A. Rolph, Cost of holographic path integrals, SciPost Phys. **14**, 061 (2023).
[42] E. Jørstad, R. C. Myers, and S.-M. Ruan, Complexity= anything: Singularity probes, J. High Energy Phys. 07 (2023) 223.
[43] S. E. Aguilar-Gutierrez, C=Anything and the switchback effect in Schwarzschild-de Sitter space, J. High Energy Phys. 03 (2024) 062.
[44] P. H. Ginsparg and M. J. Perry, Semiclassical perdurance of de Sitter space, Nucl. Phys. **B222**, 245 (1983).
[45] D. Carmi, S. Chapman, H. Marrochio, R. C. Myers, and S. Sugishita, On the time dependence of holographic complexity, J. High Energy Phys. 11 (2017) 188.
[46] L. Susskind, De Sitter space, double-scaled SYK, and the separation of scales in the semiclassical limit, arXiv:2209.09999.
[47] A. A. Rahman, dS JT gravity and double-scaled SYK, arXiv:2209.09997.
[48] A. Goel, V. Narovlansky, and H. Verlinde, Semiclassical geometry in double-scaled SYK, J. High Energy Phys. 11 (2023) 093.
[49] A. Blommaert, T. G. Mertens, and S. Yao, Dynamical actions and q-representation theory for double-scaled SYK, J. High Energy Phys. 02 (2024) 067.
[50] N. Bao, C. Cao, S. M. Carroll, and L. McAllister, Quantum circuit cosmology: The expansion of the universe since the first qubit, arXiv:1702.06959.
[51] N. Bao, C. Cao, S. M. Carroll, and A. Chatwin-Davies, De Sitter space as a tensor network: Cosmic no-hair, complementarity, and complexity, Phys. Rev. D **96**, 123536 (2017).

[52] L. Niermann and T. J. Osborne, Holographic networks for $(1 + 1)$-dimensional de Sitter space-time, Phys. Rev. D **105**, 125009 (2022).
[53] C. Cao, W. Chemissany, A. Jahn, and Z. Zimborás, Overlapping qubits from non-isometric maps and de Sitter tensor networks, arXiv:2304.02673.
[54] S. Chapman, D. A. Galante, E. Harris, S. U. Sheorey, and D. Vegh, Complex geodesics in de Sitter space, J. High Energy Phys. 03 (2023) 006.
[55] L. Aalsma, M. M. Faruk, J. P. van der Schaar, M. R. Visser, and J. de Witte, Late-time correlators and complex geodesics in de Sitter space, SciPost Phys. **15**, 031 (2023).
[56] M. A. Nielsen, A geometric approach to quantum circuit lower bounds, Quantum Inf. Comput. **6**, 213 (2006).
[57] E. K. Morvan, J. P. van der Schaar, and M. R. Visser, Action, entropy and pair creation rate of charged black holes in de Sitter space, arXiv:2212.12713.